

A Two-Process Near-Surface Downburst Wind Field Model

Matthew Mason¹

¹*School of Civil Engineering, The University of Queensland, St Lucia, Australia,*
matthew.mason@uq.edu.au

SUMMARY

A new near-surface downburst wind field model is proposed. Unlike existing models, the proposed model replicates high velocity regions associated with both the impingement and the diverging outflow front processes. The model is verified against results from a stationary downburst numerical simulation with comparisons showing the proposed model capable of reproducing the main flow features present in the radial velocity field of the numerical simulation. Future research is required to prescribe some of the inter-relationships between model variables currently assumed to be independent.

Keywords: downbursts, microburst, thunderstorm

1. INTRODUCTION

Two main types of downburst wind field model are generally used by the wind engineering community. The first is based upon the concept of a steady impinging jet. The premise of this model is founded in atmospheric observations, with early downburst research linking the divergent wind field observed in nature with laboratory experiments using a steady impinging jet (Hjelmfelt, 1988). The second type of model is based upon the mathematics of ring vortices and their interaction with a surface (Jesson and Sterling, 2018). Both types of model replicate aspects of downbursts – and here we are primarily referring to microbursts – but neither captures all potential high velocity wind regions that may be of interest to a wind engineer.

Observational (Hjelmfelt, 1988), experimental (Alahyari and Longmire, 1988) and numerical (Mason et al., 2010) studies have shown that two main high velocity regions exist within the near-surface wind field of a downburst outflow (Figure 1). The first being the impingement region, which sits just outside the descending downdraft and adjacent to a high-pressure stagnation region, or meso-high. The second is beneath the diverging outflow front. While the high velocity impingement region remains located outside the downdraft throughout a storm, the high velocity region below the outflow front diverges as the outflow itself radiates away from the downdraft.

The widely used near-surface impinging jet-based downburst wind field model of Holmes and Oliver (2000) models the high wind speed region associated with impingement but not the diverging front region. Xhelaj et al. (2021), among others, have proposed modifications to this model to enable more of the transient downburst features to be incorporated but none of these explicitly model the high velocity region at the leading edge of the front. In contrast, ring vortex

models simulate a diverging and stretching ring vortex, which is generally assumed to be the primary flow feature associated with the front. Models such as Jesson and Sterling (2018) provide an approach to model the three-dimensional wind field associated with this region, but they ignore the high velocity winds associated with downdraft impingement.

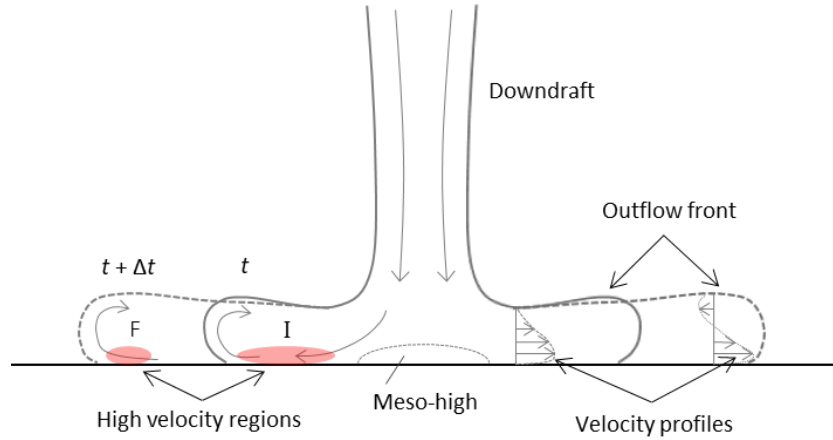


Figure 1. Conceptual model of downdraft outflow event showing the regions of high wind velocity (*I*: impingement and *F*: outflow front) and the divergence of the outflow with time, *t*. After Mason (2017).

Given the limitations discussed, the aim of this research is to develop a near-surface downburst wind field model that can replicate winds in both the high velocity region associated with impingement and the outflow front. The following section will describe the proposed model with the subsequent section comparing model output with idealised numerical simulation results.

2. NEAR-SURFACE WIND FIELD MODEL

The proposed model models the two high velocity regions as separate (but linked) processes, with the resulting wind field simply being the summation of the two. That is, for a stationary axisymmetric downburst, the near-surface divergent wind velocity at any location r from the centre of the downdraft can be calculated by summing velocities from an impingement region velocity model, V_I , and a model of the velocities within the diverging front, V_F . Equations for V_I and V_F are given in Eq. (1) – (5). The equations used to model the impingement region flow, i.e. V_I , are a slightly modified version of those presented in Holmes and Oliver (2000), with the winds within the radius of maximum winds, r_I , modelled here as a non-linear function of r so that the transition at r_I is smoother than in the original linear form of the model. V_F is modelled as a translating soliton and is mathematically represented using the hyperbolic secant function with variable shape parameters, $R_F = R_{F,i}$ or $R_{F,o}$, on either the inner or outer side of its peak at r_F . The magnitude of both V_I and V_F is time dependent through the intensity functions Π_I and Π_F with the location of r_I and r_F also time dependent. The impingement region velocity decay constant, R_I is used to link the impingement region and front velocity functions through Eq. (4). This equation forces the location of r_F to match the point on Eq. (2) where $V_R = \lambda V_{I,max}$. A matching parameter of $\lambda = 0.1$ is used here and appears to be reasonable, but further research is required to confirm this.

$$V_R = V_I + V_F \quad (1)$$

$$\begin{aligned}
V_I &= V_{I,max} \Pi_I \left(1 - \left(1 - \frac{r}{r_I} \right)^2 \right) \quad \text{for } r < r_I \\
&= V_{I,max} \Pi_I e^{-\left(\frac{r-r_I}{R_I} \right)^2} \quad \text{for } r \geq r_I
\end{aligned} \tag{2}$$

$$V_F = V_{F,max} \Pi_F \operatorname{sech} \left(\frac{r-r_F}{R_F} \right) \tag{3}$$

$$R_I = \frac{r_F - r_I}{\sqrt{-\ln(\lambda)}} \tag{4}$$

$$V_{F,max} = V_{F,total} - \lambda V_{I,max} \tag{5}$$

Figure 2 shows examples of the model output for a stationary downburst at two conceptual points in time. Figure 2 (a) shows a profile at a time shortly after impingement where the front is generating the maximum storm winds as it begins to diverge away from the impingement region. Figure 2 (b) shows a time after the front has moved well away from the downdraft and the impingement region produces the storm maximum winds. The relative components of V_I and V_F and the resulting radial velocity V_R are shown.

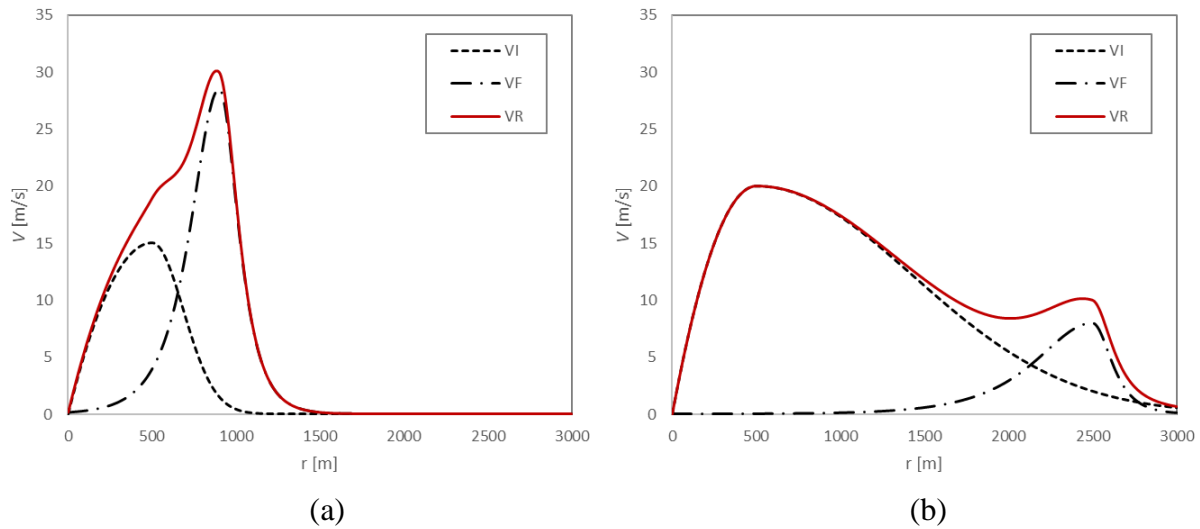


Figure 2. Examples of the near-surface radial wind velocity generated by the model (a) shortly after downdraft impingement, and (b) after the outflow front has diverged away from the downdraft.

While the model is currently formulated with all variables treated independently, in reality, many can be linked empirically, through theory or by reasoning. Specific examples of this could be the decay of $V_{F,max}$ with increase in r_F or the relationship between Π_I and Π_F throughout the storm evolution. Research is underway to describe these (and more) linkages and will be reported in the presentation.

3.0 MODEL VERIFICATION

To assess whether the proposed model can generate realistic near-surface wind fields, wind velocities at an elevation of 10 m were extracted at four instants in time from the stationary downburst simulation described in Mason et al. (2010). Figure 3 shows the simulated velocities as markers and the solid lines show the model fit to these data. The proposed model is shown capable of generating most of the flow features at each of the extracted simulation time steps, with the only major discrepancies occurring near the leading edge of the front where in the numerical simulations a counter rotating secondary vortex influences the local velocities. Given this, the functional form of the model proposed here appears to be suitable for replicating the time-dependent near-surface downburst velocity field of a stationary downburst. However, research is still required to determine and implement relationships between model variables and to also incorporate other storm or environmental attributes such as storm motion or environmental winds.

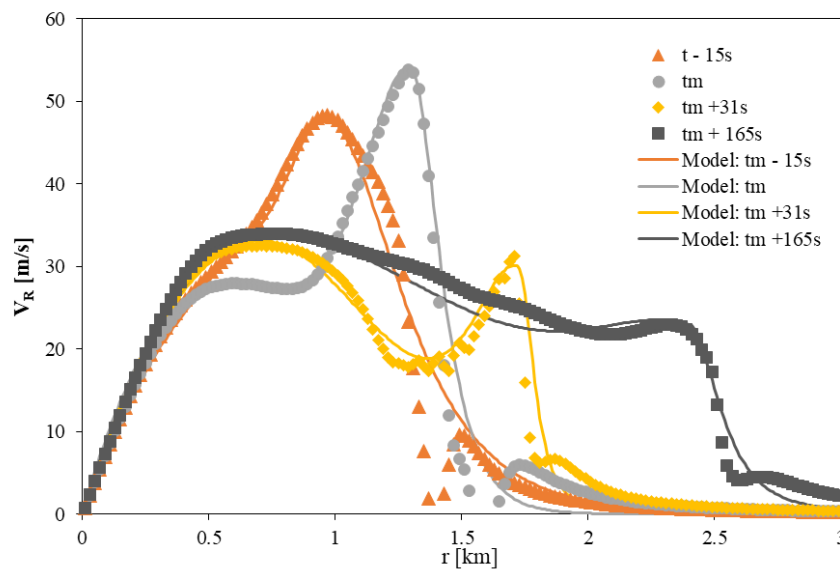


Figure 3. Near-surface radial wind velocities for a simulated stationary downburst (markers) and model fitting to those data. tm is the time of maximum velocity in the numerical simulation.

REFERENCES

- Alahyari, A. and Longmire, E.K., 1995. Dynamics of experimentally simulated microbursts. *AIAA Journal*, 33, 2128-2136.
- Hjelmfelt, M.R., 1988. Structure and life cycle of microburst outflows observed in Colorado. *Journal of Applied Meteorology*, 27, 900-927.
- Holmes, J.D. and Oliver, S.E., 2000. An empirical model of a downburst. *Engineering Structures*. 22, 1167-1172.
- Jesson, M. and Sterling, M., 2018. A simple vortex model of a thunderstorm downburst – A parametric evaluation. *Journal of Wind Engineering and Industrial Aerodynamics*. 174, 1-9.
- Mason, M.S., Fletcher, D.F., Wood, G.S., 2010. Numerical simulation of idealized three-dimensional downburst wind fields. *Engineering Structures*. 32, 3558-3570.
- Mason, M.S., 2017. Towards codification of localized windstorms: Progress and challenges. *Proceedings of the 9th Asia-Pacific Conference on Wind Engineering*, 3-7 December, Auckland, New Zealand.
- Xhelaj, A., Burlando, M., Solari, G., 2020. A general-purpose analytical model for reconstructing the thunderstorm outflows of travelling downbursts immersed in ABL flows. *Journal of Wind Engineering and Industrial Aerodynamics*. 207, 104373.